Durability and Reliability of Materials and Components for SOFC

Edgar Lara-Curzio, Michael Lance, Qianying Guo, Alexis Flores-Betancourt, Beth Armstrong, Alex Rogers, Antonio Macias, Kinga Unocic

2020 SOFC Program Review

Outline

- Development of model to explain anomalous thermal dependence of residual stresses in SOFCs
- Microstructural characterization of multi-component silicate glasses
- Additive manufacturing of SOFC materials and structures
- Summary

Lara-Curzio et al. (2020)

Development of model to explain anomalous thermal dependence of residual stresses in SOFCs

- ORNL has measured the state of residual stresses in SOFC materials and components using various techniques, including X-ray diffraction, Raman spectroscopy, DIC.
- X-ray diffraction measurements of bilayers (NiO-YEZ/YSZ) have shown a non-linear temperature dependence of the residual stresses.
- A model that accounts for phase transitions of NiO at the Neel temperature and order-disorder transitions of YSZ has been developed to accurately explain the anomalous behavior.

Lara-Curzio et al. (2020)

Residual Stresses in SOFCs

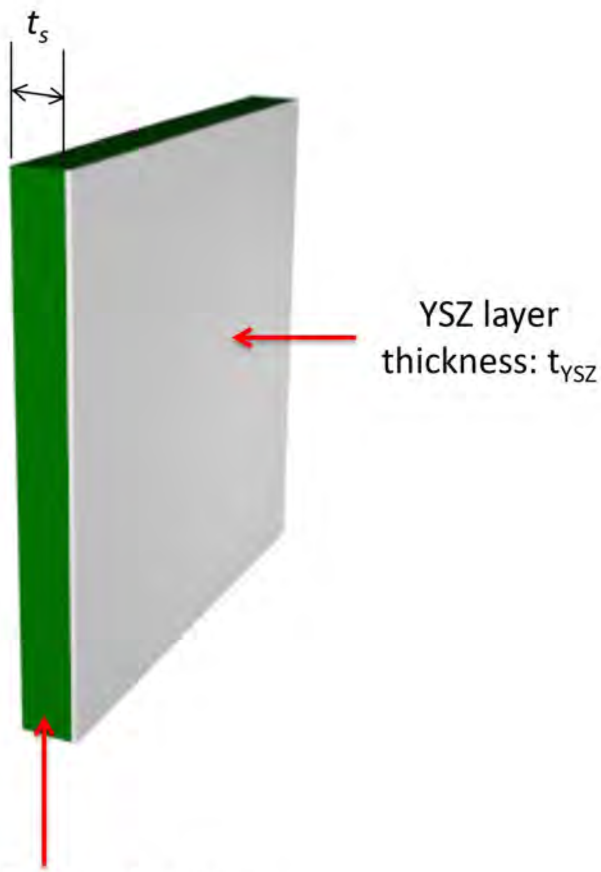

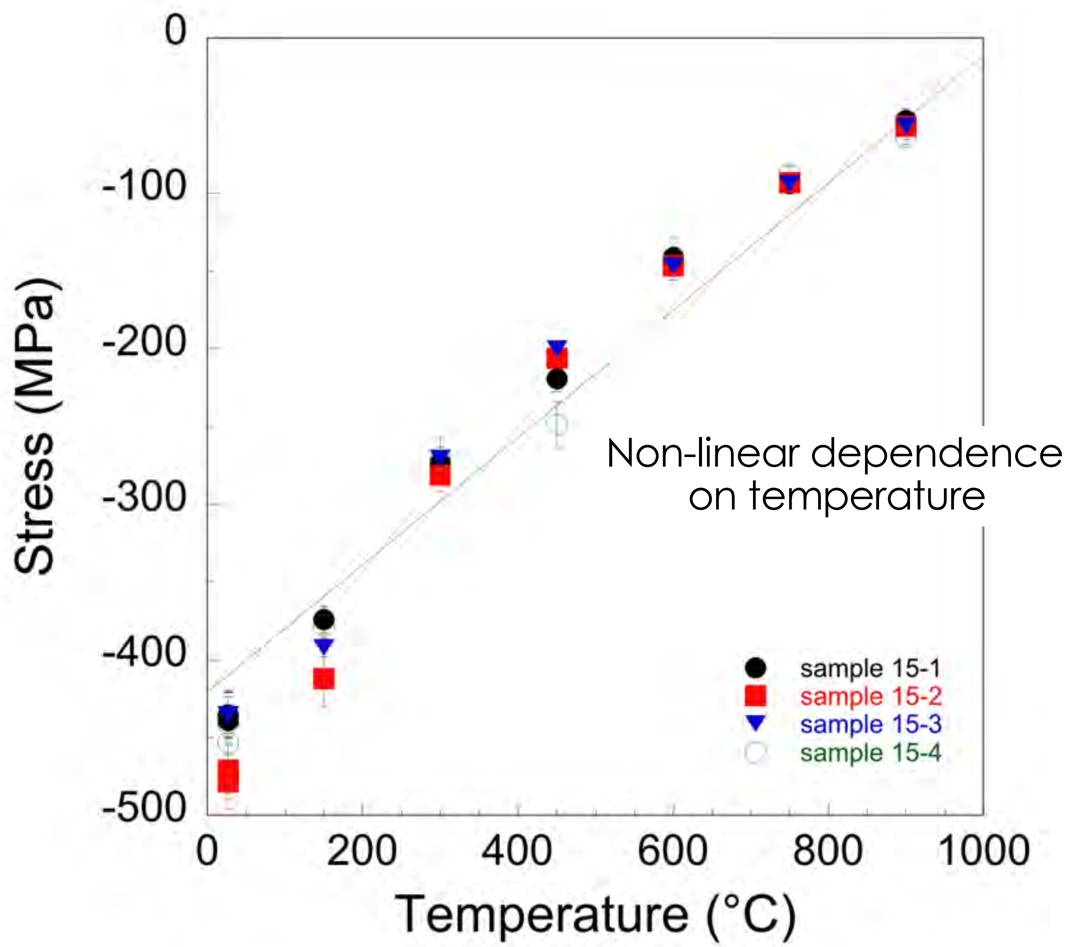

Lara-Curzio et al. (2020)

Submitted for publication Journal of the American Ceramic Society (2020)

Determination of Residual Stresses by X-Ray Diffraction

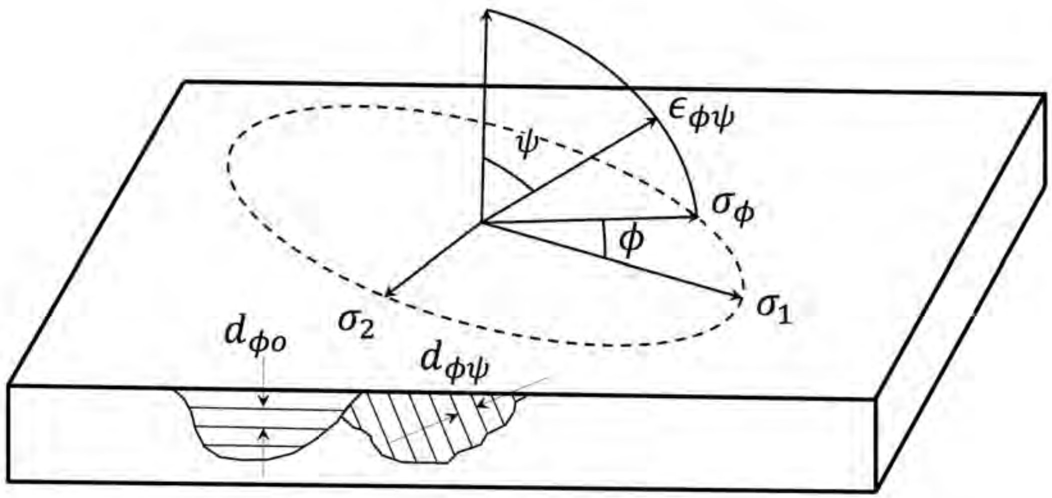

$$\epsilon_{\phi\psi} = \frac{1+\nu}{E}\sigma_\phi \sin^2\psi - \frac{\nu}{E}(\sigma_1 + \sigma_2)$$

$$\epsilon_{\phi\psi} = \frac{d_{\phi\psi} - d_o}{d_o}$$

d_o is the stress-free lattice spacing and $d_{\phi\psi}$ is the spacing between lattice planes measured in the direction defined by ϕ and ψ. Values of d_o are determined when $\psi = 0$.

The peak of interest was the (620) reflection of YSZ, which was found in the 2θ = 141°-145° range. The maximum value of ψ was 55° and the sample was tilted in 7 equal steps of $Sin^2\,\psi$ (both positive and negative tilts). From the slope of a plot of $\epsilon_{\phi\psi}$ $vs.$ $\sin^2\psi$, we obtain the value of the equibiaxial residual stress on the surface of the specimen

Lara-Curzio et al. (2020)

NiO-YSZ anodes are 3-phase composites

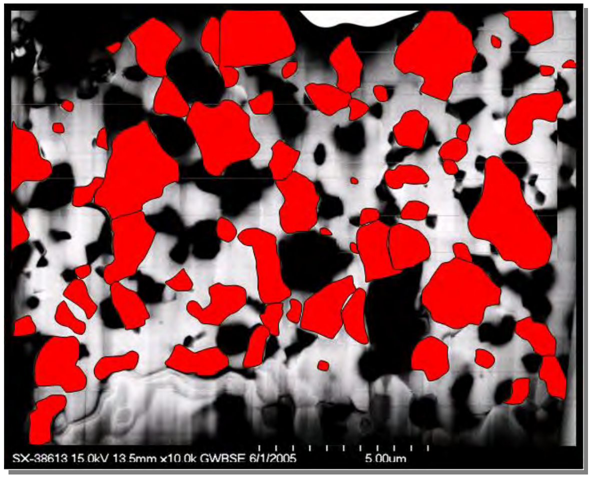

Lara-Curzio et al. (2020)

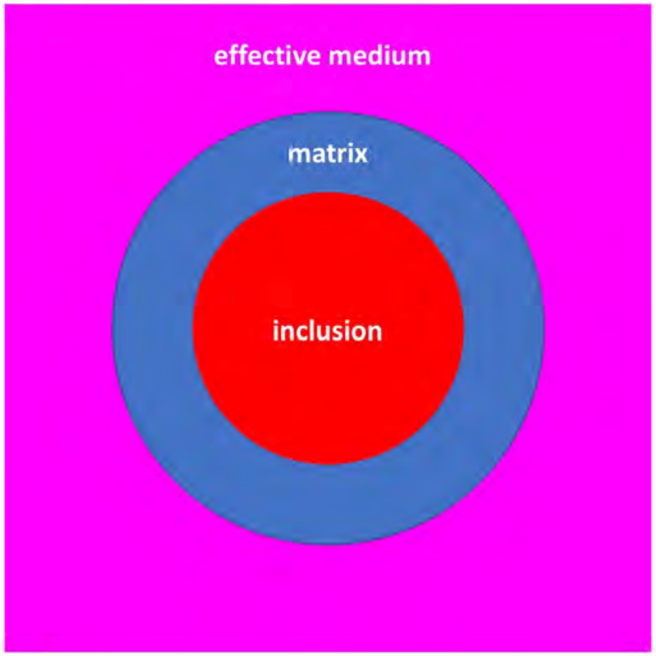

A micromechanics model has been developed to calculate the effective properties of a 3-phase composite (NiO, YSZ and porosity) as a function of temperature.

Submitted for publication Journal of the American Ceramic Society (2020)

Elastic Moduli of YSZ

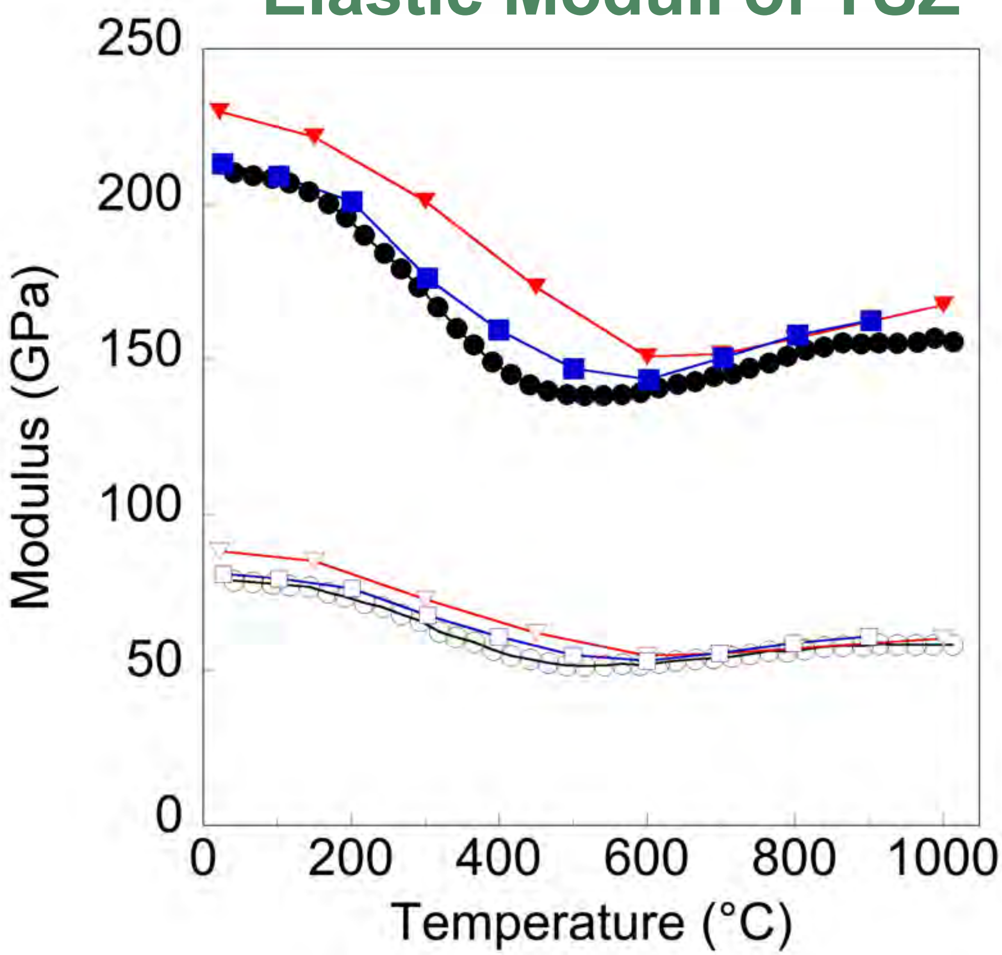

Lara-Curzio et al. (2020)

Triangles are data from: Radovic M, Lara-Curzio E, Trejo RM, Wang H, and Porter WD. “Thermo-Physical Properties of Ni-YSZ as a Function of Temperature and Porosity,” *Ceramic Engineering and Science Proceedings*, **27**, Issue 4 (2006) pp. 79-85.; **squares** from: Gao P, Bolon A, Taneja M, Xie Z, Orlovskaya N, and Radovic M. “Thermal expansion and elastic moduli of electrolyte materials for high and intermediate temperature solid oxide fuel cell,” *Solid State Ionics* **300** (2017) 1–9; circles are from: Kushi T, Sato K, Unemoto A, Hashimoto S, Amezawa K, and Kawada T. “Elastic modulus and internal friction of SOFC electrolytes at high temperatures under controlled atmospheres,” *Journal of Power Sources*, **Vol. 196**, Issue 19, pp. 7989-7993 (2011).

Open symbols correspond to values of shear modulus, whereas closed symbols correspond to values of Young’s modulus.

Anomalous Young's Modulus of NiO

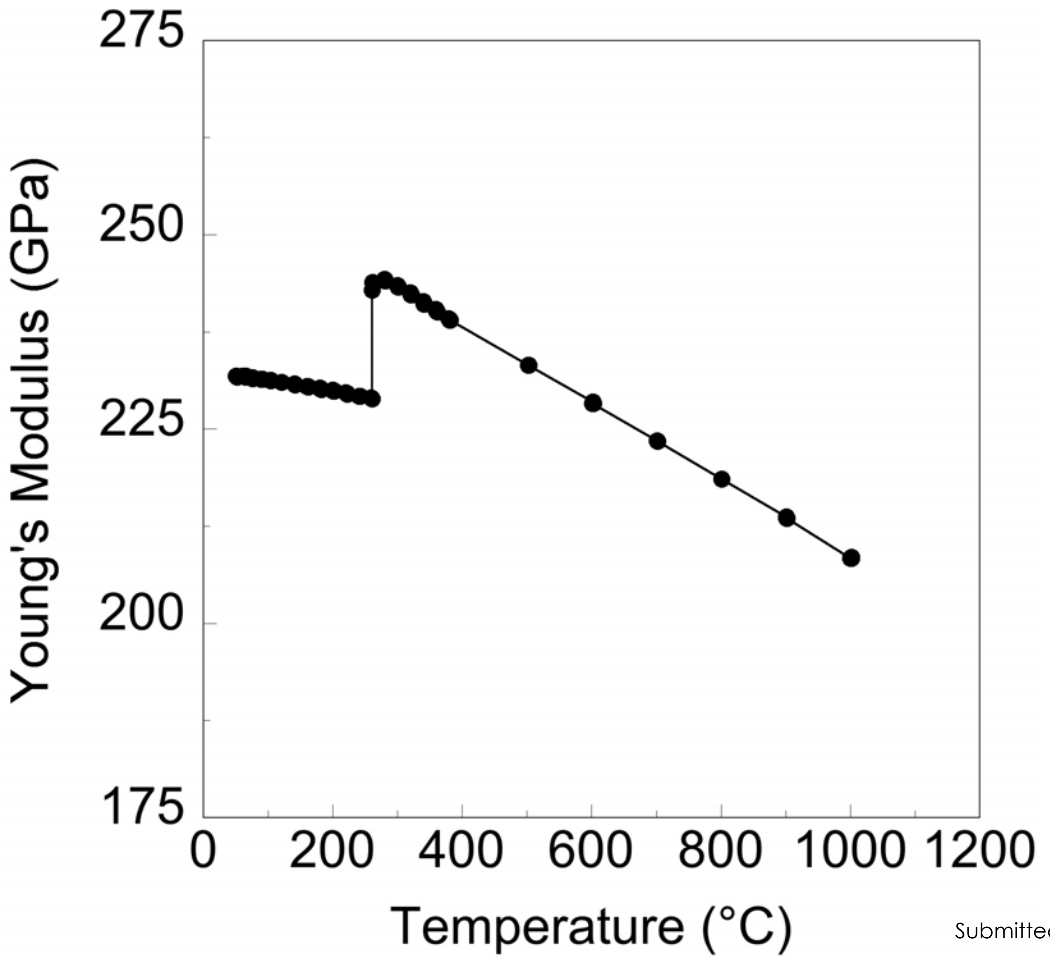

Young's modulus of NiO determined by impulse excitation as a function of temperature.

Submitted for publication Journal of the American Ceramic Society (2020)

Thermal Expansion Behavior of NiO

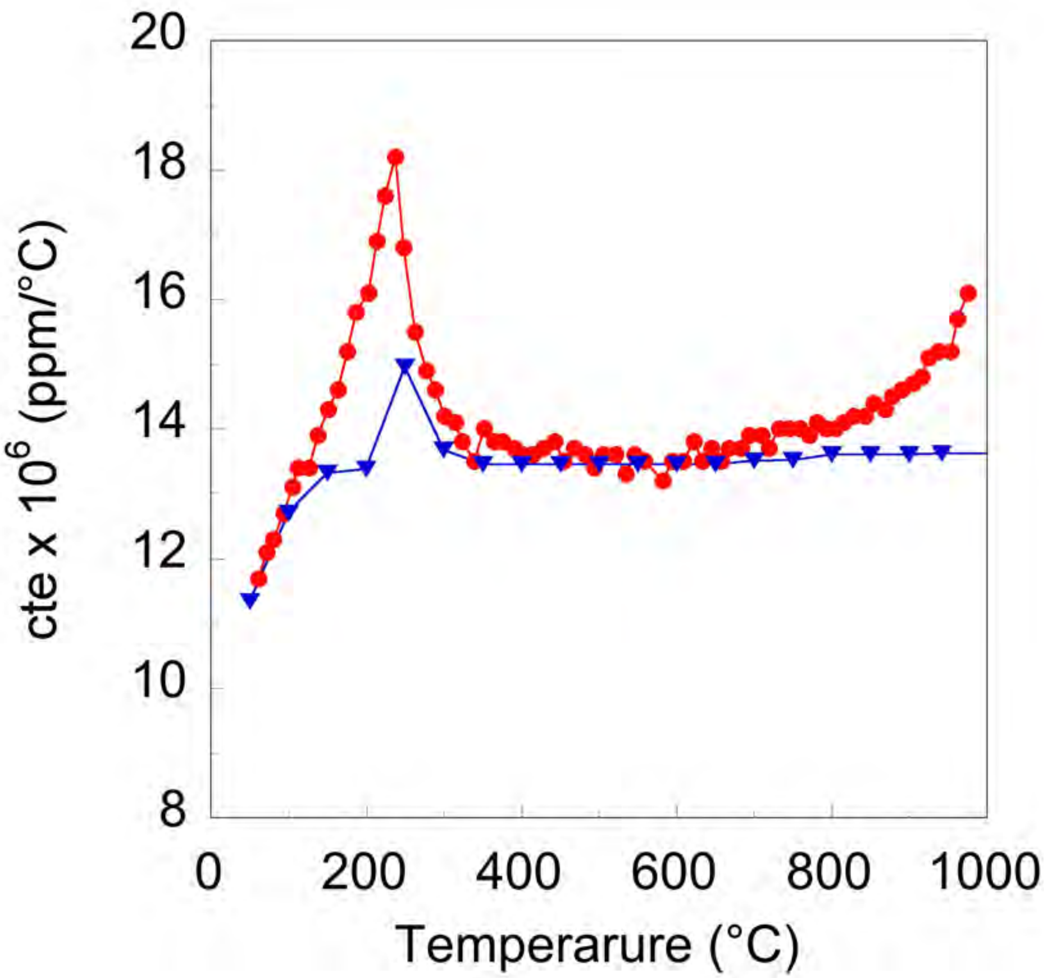

Coefficient of thermal expansion of NiO. **Blue triangles** from: CINDAS LLC, Purdue Technology Center- Aerospace, 1801 Newman Road, Suite 104B, West Lafayette, IN 47906-4510. **Red circles** from: Mori M, Yamamoto T, Itoh H, Inaba H, and Tagawa H. "Thermal Expansion of Nickel-Zirconia Anodes in Solid Oxide Fuel Cells during Fabrication and Operation," *J. Electrochem. Soc.*, **Vol. 145**, No.4, April 1998 pp.1374-1381.

Note the abrupt change at the Neél temperature

Submitted for publication Journal of the American Ceramic Society (2020)

Determination of Residual Stresses n Multilayers

$$\sigma_s = \frac{E_s}{1-\nu_s}(\varepsilon - \alpha_s \Delta T)$$

$$\xi = \frac{\frac{E_S(T)}{(1-\nu_S(T))} t_S \int_{T1}^{T2} \alpha_S(T)dT + \frac{E_{YSZ}(T)}{(1-\nu_{YSZ}(T))} t_{YSZ} \int_{T_2}^{T_2} \alpha_{YSZ}(T)\,dT}{\frac{E_S(T)}{(1-\nu_S(T))} t_S + \frac{E_{YSZ}(T)}{(1-\nu_{YSZ}(T))} t_{YSZ}}$$

$$\sigma_{YSZ} = \frac{E_{YSZ}}{1-\nu_{YSZ}}(\varepsilon - \alpha_{YSZ} \Delta T)$$

$$t_b = \frac{\frac{E_{YSZ}(T)}{(1-\nu_{YSZ}(T))} t_{YSZ}^2 - \frac{E_S(T)}{(1-\nu_S(T))} t_S^2}{2\left(\frac{E_S(T)}{(1-\nu_S(T))} t_S + \frac{E_{YSZ}(T)}{(1-\nu_{YSZ}(T))} t_{YSZ}\right)}$$

$\varepsilon = \xi + \frac{z-t_b}{r}$ (for $t_s \le z \le t_{YSZ}$)

$$\frac{1}{r} = \frac{6\, t_S\, t_{YSZ}\,(t_S + t_{YSZ}) \frac{E_S(T)\, E_{YSZ}(T)}{(1-\nu_S(T))(1-\nu_{YSZ}(T))} \int_{T_1}^{T_2} (\alpha_{YSZ}(T) - \alpha_S(T))dT}{\frac{E_S^2(T)}{(1-\nu_S(T))^2} t_S^4 + \frac{E_{YSZ}^2(T)}{(1-\nu_{YSZ}(T))^2} t_{YSZ}^4 + 2\frac{E_S(T)\, E_{YSZ}(T)}{(1-\nu_S(T))(1-\nu_{YSZ}(T))} t_S\, t_{YSZ}\,(2t_S^2 + 2t_{YSZ}^2 + 3\, t_S\, t_{YSZ})}$$

Adapted from: Hsueh CH. “Thermal stresses in elastic multilayer systems,” *Thin Solid Films* **418** (2002) 182–188.

Lara-Curzio et al. (2020)

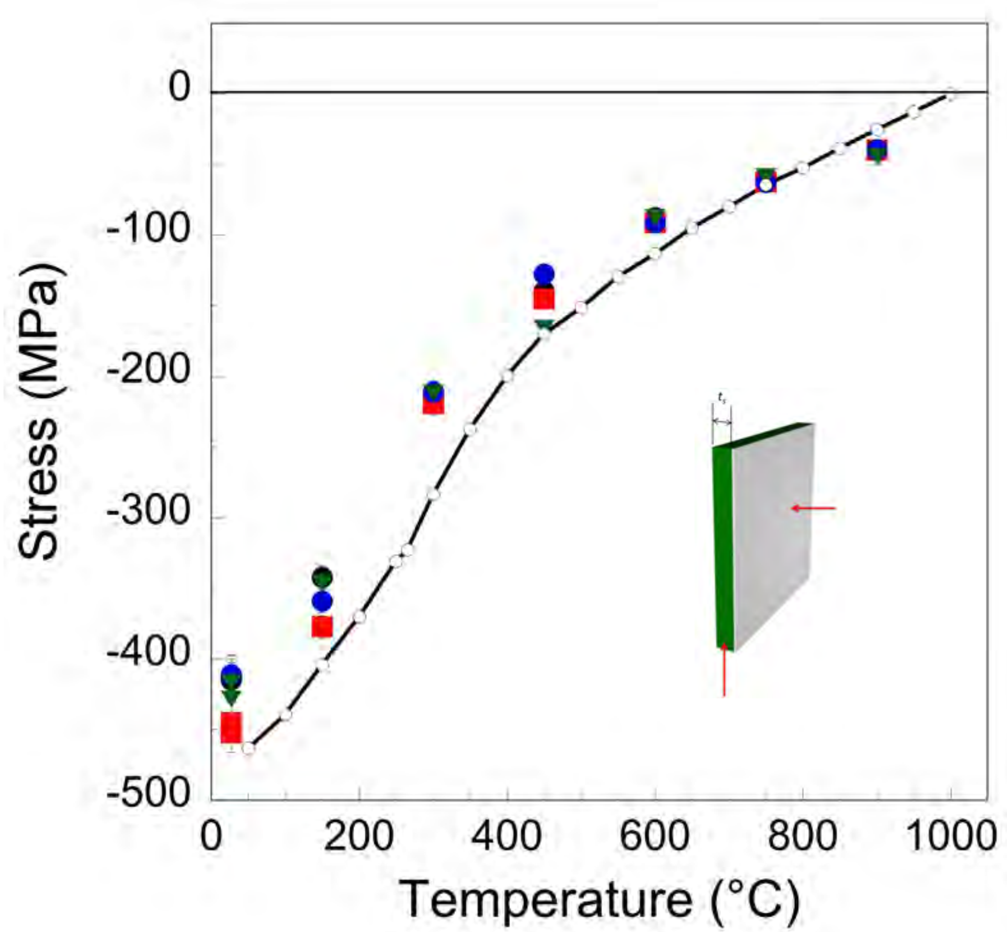

Lara-Curzio et al. (2020)

Residual Stresses in SOFCs

- State of residual stresses in YSZ layer. The continuous curve corresponds to model predictions, which captures the effect of transitions in NiO and YSZ.
- Data points correspond to residual stress values determined by X-ray diffraction on the YSZ surface of NiO-YSZ/YSZ bilayers. Color distinguishes between values obtained from different test specimens originating from the same sample.

Submitted for publication Journal of the American Ceramic Society (2020)

Microstructural characterization of multi-component silicate glasses

- ORNL is characterizing the evolution of the microstructure of multi-component silicate glasses for SOFC sealing applications.
- Two commercially-available glasses are being investigated: SCN and G6
- Glass samples were mounted on either YSZ or Al_2O_3 substrates, and exposed at 800°C to air or gas mixtures of H_2+H_2O+N_2 for up to 40,000 hours.
- A combination of techniques, that include Raman spectroscopy, X-ray diffraction, electron microprobe and scanning electron microscopy have been used.

Lara-Curzio et al. (2020)

Electron microprobe analysis of glasses

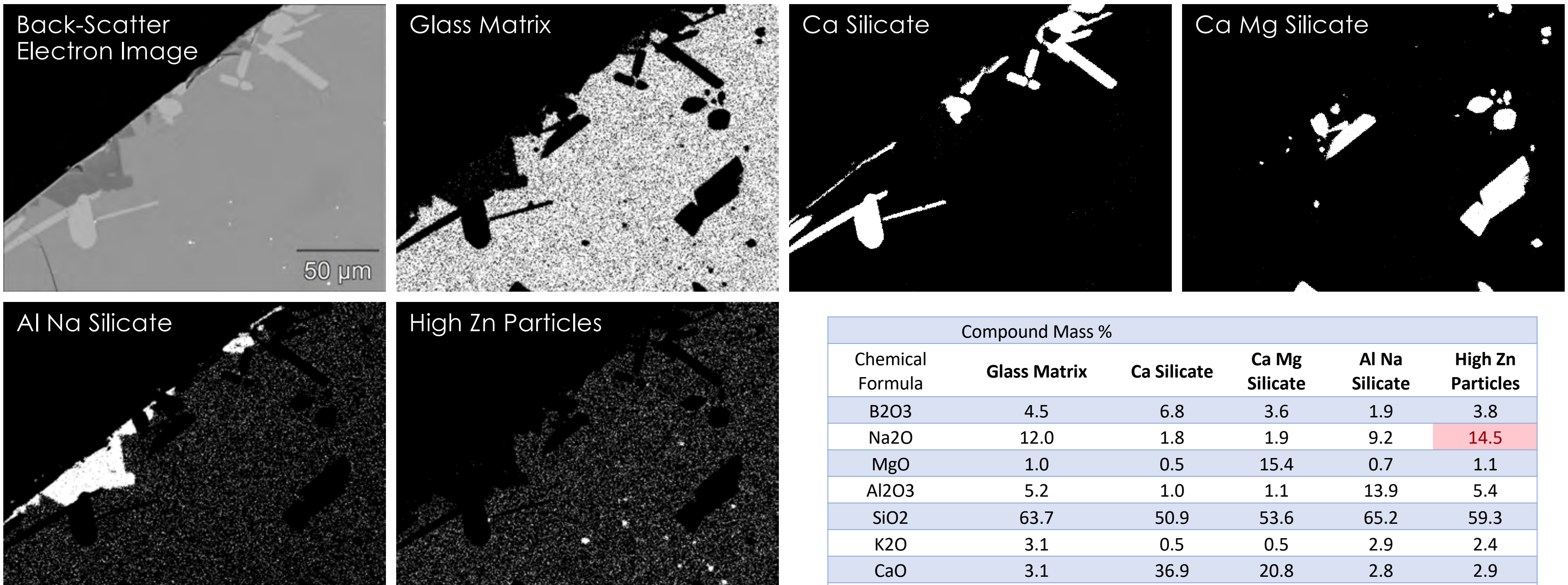

Compound Mass %					
Chemical Formula	**Glass Matrix**	**Ca Silicate**	**Ca Mg Silicate**	**Al Na Silicate**	**High Zn Particles**
B2O3	4.5	6.8	3.6	1.9	3.8
Na2O	12.0	1.8	1.9	9.2	14.5
MgO	1.0	0.5	15.4	0.7	1.1
Al2O3	5.2	1.0	1.1	13.9	5.4
SiO2	63.7	50.9	53.6	65.2	59.3
K2O	3.1	0.5	0.5	2.9	2.4
CaO	3.1	36.9	20.8	2.8	2.9
Fe2O3	0.2	0.1	0.6	0.1	0.0
ZnO	3.1	0.7	2.1	1.5	6.9
BaO	4.2	0.8	0.6	1.7	3.8

G6 glass on alumina after 10,000 hrs in H_2+H_2O+N_2.

Lara-Curzio et al. (2020)

Electron microprobe analysis of glasses

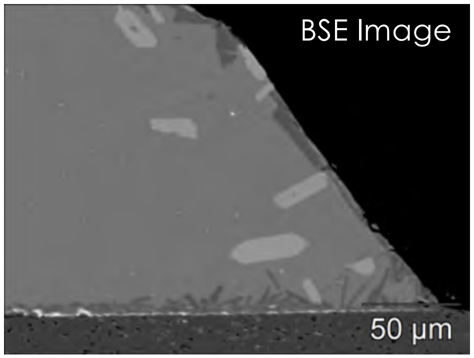

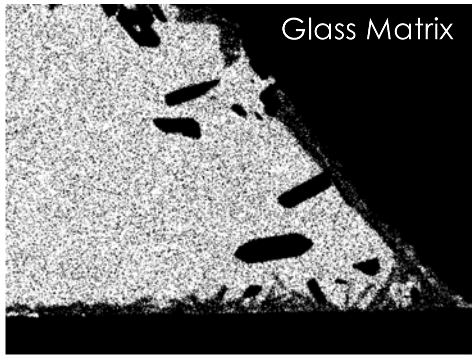

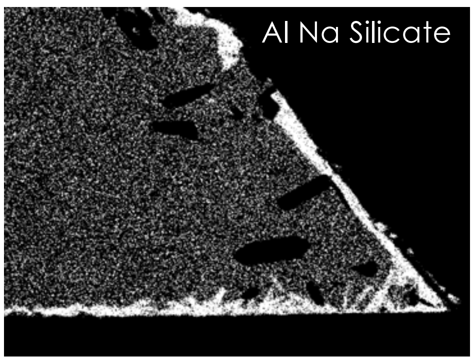

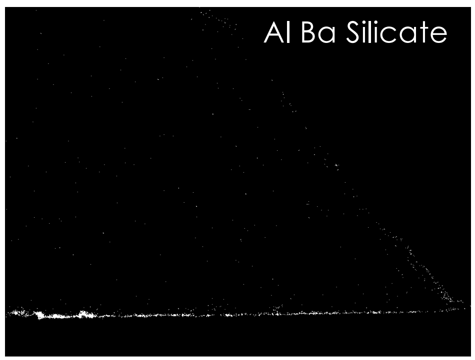

	Compound Mass %				
Chemical Formula	**Glass Matrix**	**Ca Silicate**	**Ca Mg Silicate**	**Al Na Silicate**	**Al Ba Silicate?**
B2O3	4.7	5.2	4.8	1.9	4.8
Na2O	13.0	1.2	2.8	8.1	6.4
MgO	1.0	0.5	14.0	0.7	0.3
Al2O3	5.5	0.8	2.2	10.5	29.6
SiO2	61.9	51.3	53.9	70.2	41.7
K2O	2.8	0.4	0.7	3.7	2.6
CaO	2.8	38.9	17.8	2.1	0.5
Fe2O3	0.1	0.1	0.6	0.3	0.1
ZnO	4.1	0.9	2.4	1.0	1.5
BaO	4.2	0.8	0.8	1.4	12.5

G6 glass on alumina after 10,000 hrs in H_2+H_2O+N_2.

Lara-Curzio et al. (2020)

Electron microprobe analysis of glasses

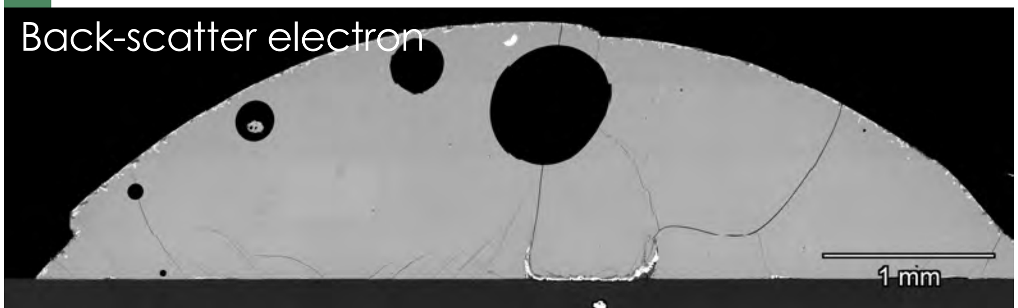

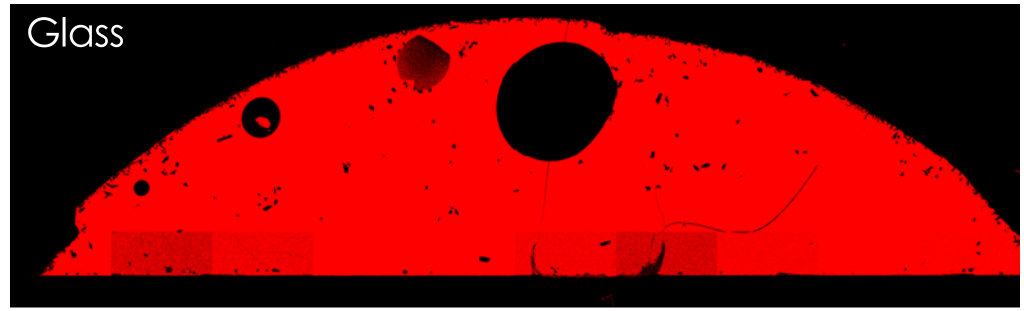

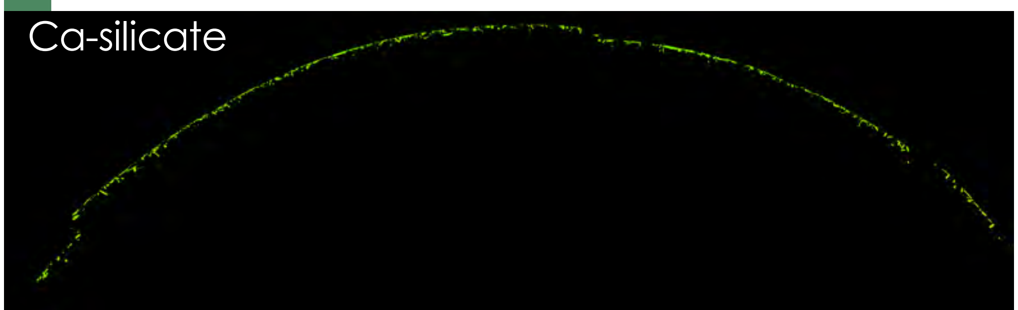

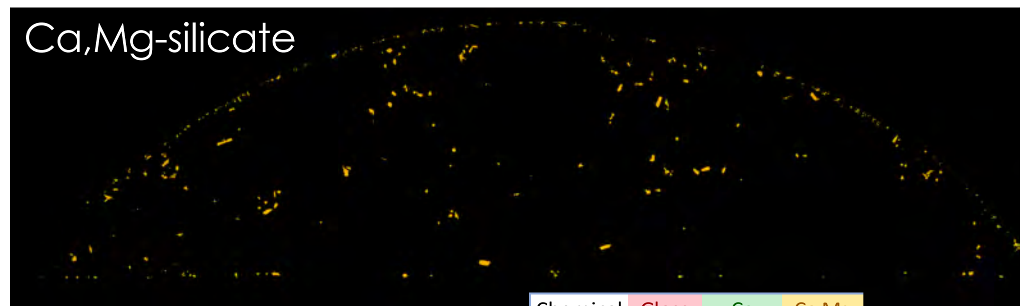

Chemical Formula	Glass Matrix	Ca Silicate	Ca Mg Silicate
B2O3	4.5	6.8	3.6
Na2O	12.0	1.8	1.9
MgO	1.0	0.5	15.4
Al2O3	5.2	1.0	1.1
SiO2	63.7	50.9	53.6
K2O	3.1	0.5	0.5
CaO	3.1	36.9	20.8
Fe2O3	0.2	0.1	0.6
ZnO	3.1	0.7	2.1
BaO	4.2	0.8	0.6

Wt%

G6 glass on alumina after 10,000 hrs in H_2+H_2O+N_2.

Lara-Curzio et al. (2020)

BSE images and EDS maps at SCN-Al_2O_3 interface region

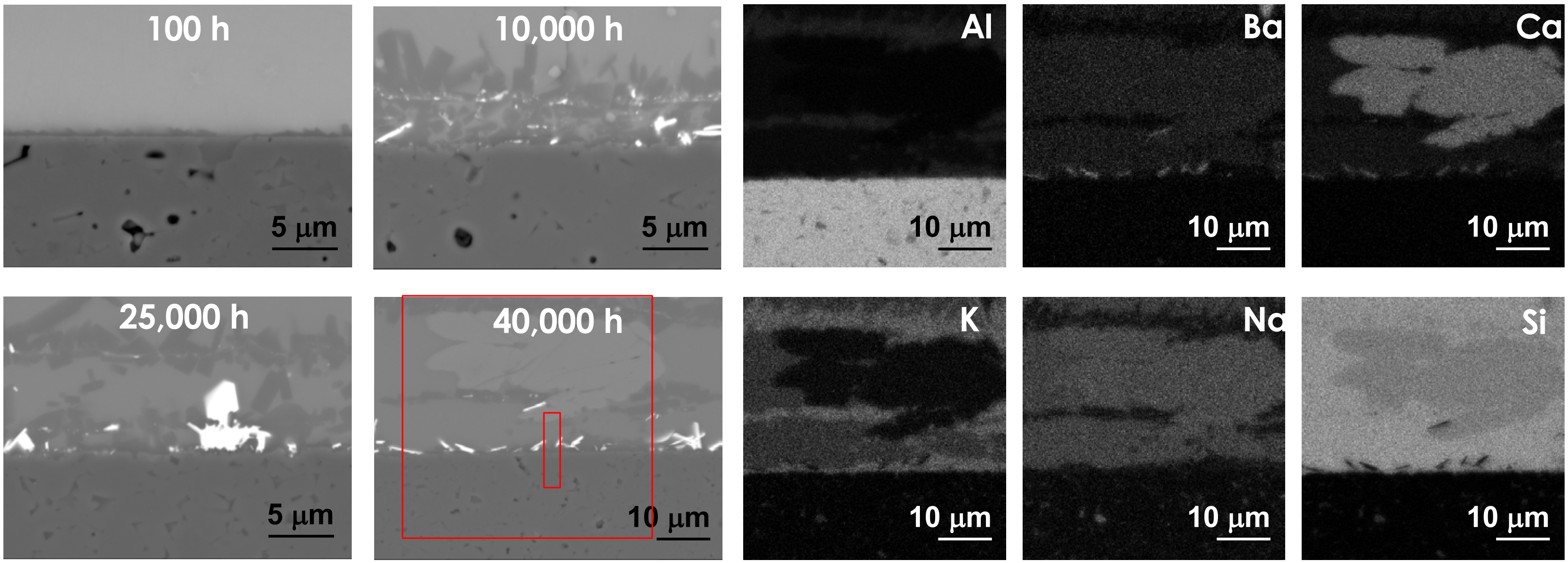

Structure and chemical changes at interfaces region by using SEM – three new phases formed at the SCN-Al2O3 interface. Ba-Ca-O based (bulk in center), Ba-Si-O based (bright lath), and K-Al-Si-O based (dark lath);. GB diffusion in substrate was apparent.

Lara-Curzio et al. (2020)

BSE images and EDS maps at G6-Al_2O_3 interface region

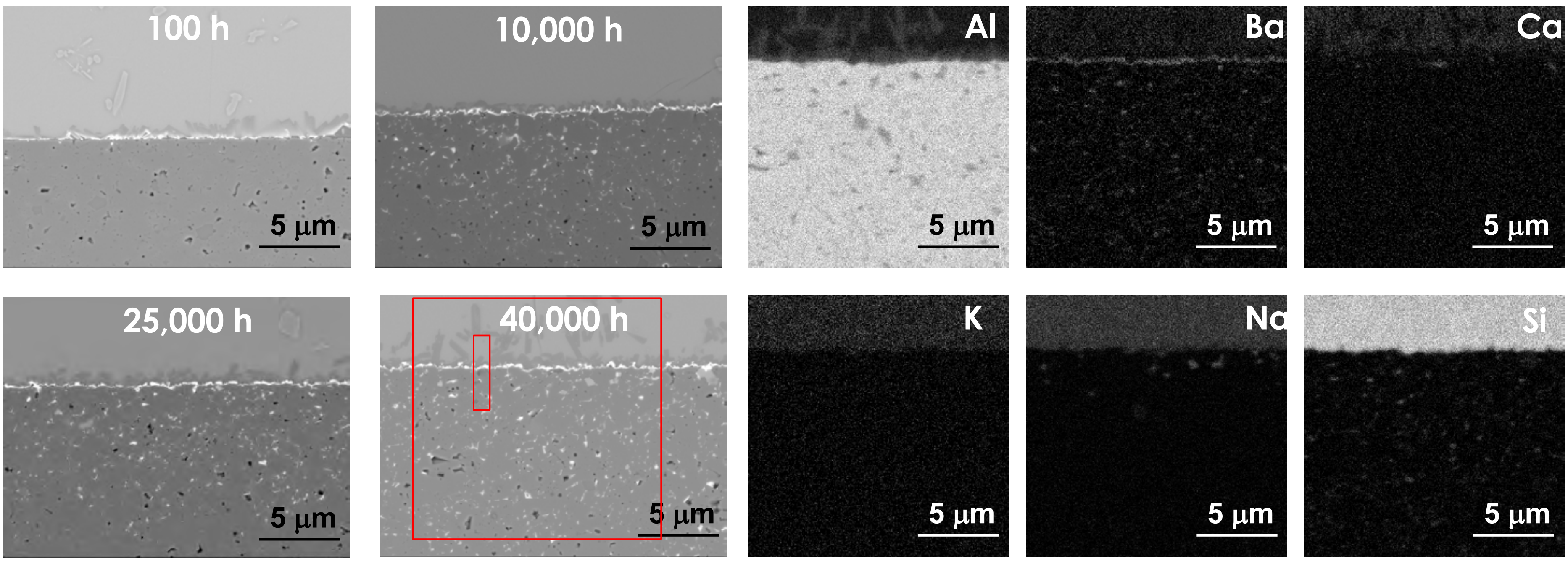

Structure and chemical changes at interfaces region by using SEM – two new phases formed at the G6-Al2O3 interface: Al-Na-Si-O based (dark lath at interface) and Ba-Al-Si-O based (thin bright layer). Significant GB diffusion was noted.

Lara-Curzio et al. (2020)

Interphase thickness as a function of time

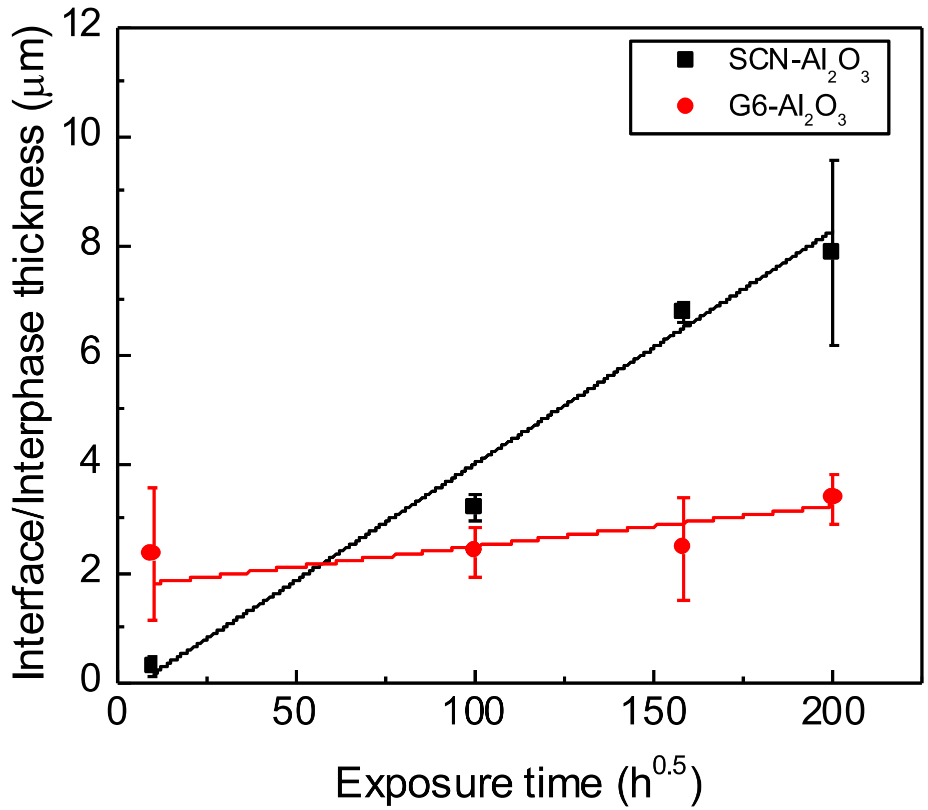

Results suggest diffusion controlled process

Lara-Curzio et al. (2020)

Interphase thickness as a function of time

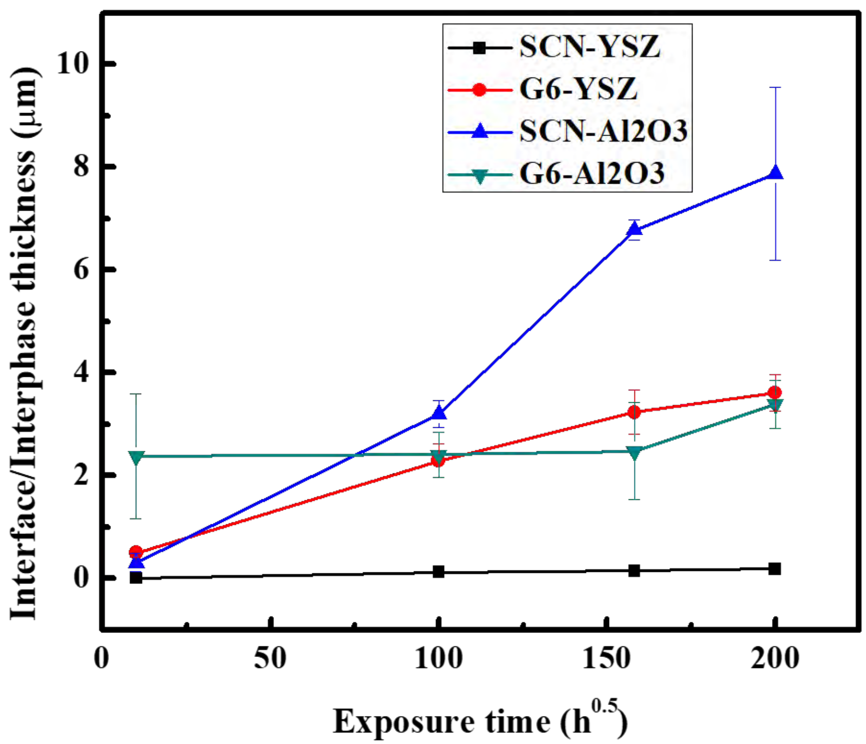

Lara-Curzio et al. (2020)

Region of Analysis

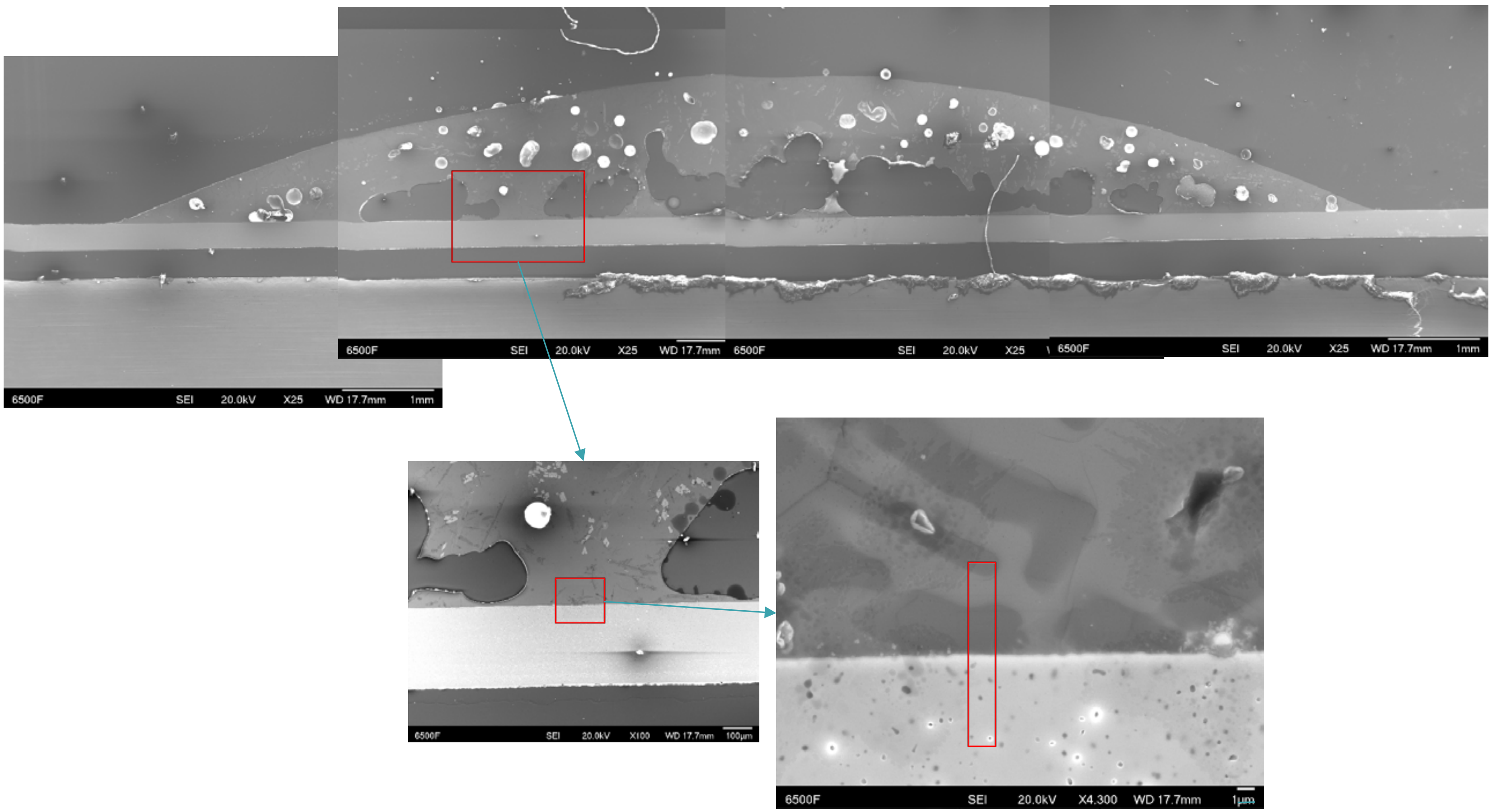

Lara-Curzio et al. (2020)

SCN-YSZ 25k Sub/Glass interface

STEM-EDS: Overview

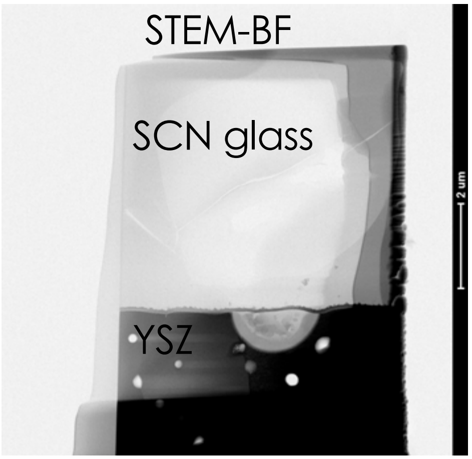

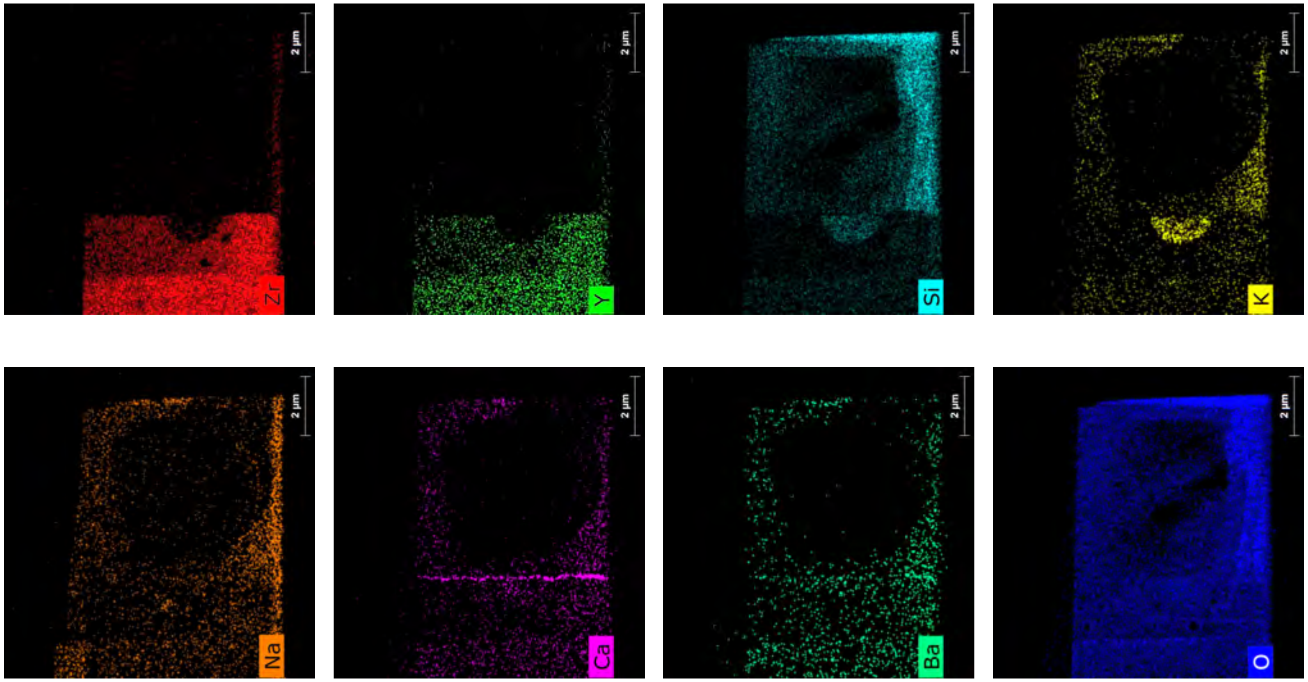

Substrate: Zr-Y-O with a half sphere void with Si-K

Interphase/layer: Ca-Ba-Si-O

Need high magnification to verify

Lara-Curzio et al. (2020)

Phase transformation of YSZ at interfacial region – Raman analysis

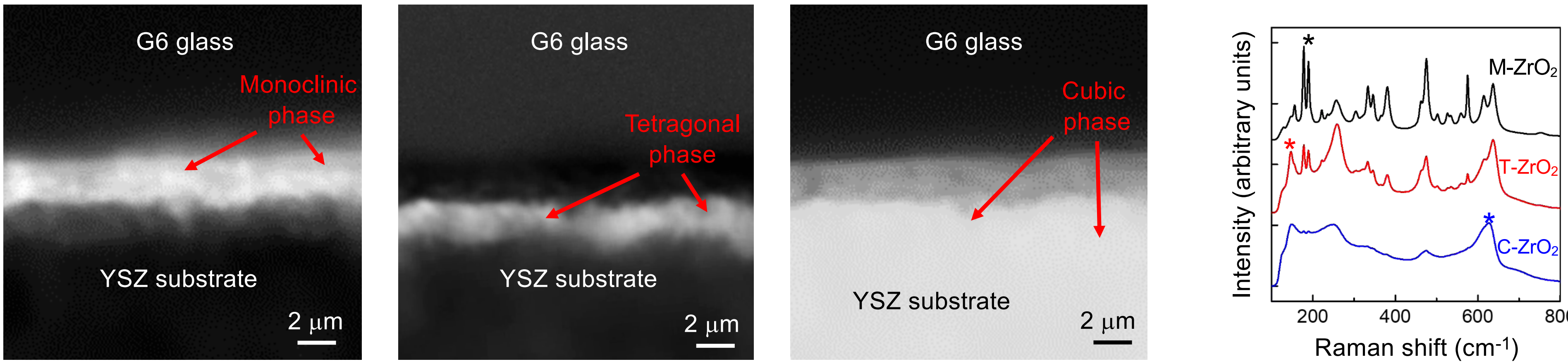

Lara-Curzio et al. (2020)

Raman spectroscopy was used to detect phase transformation of the G6 glass on an 8YSZ substrate after 40,000 hours in air

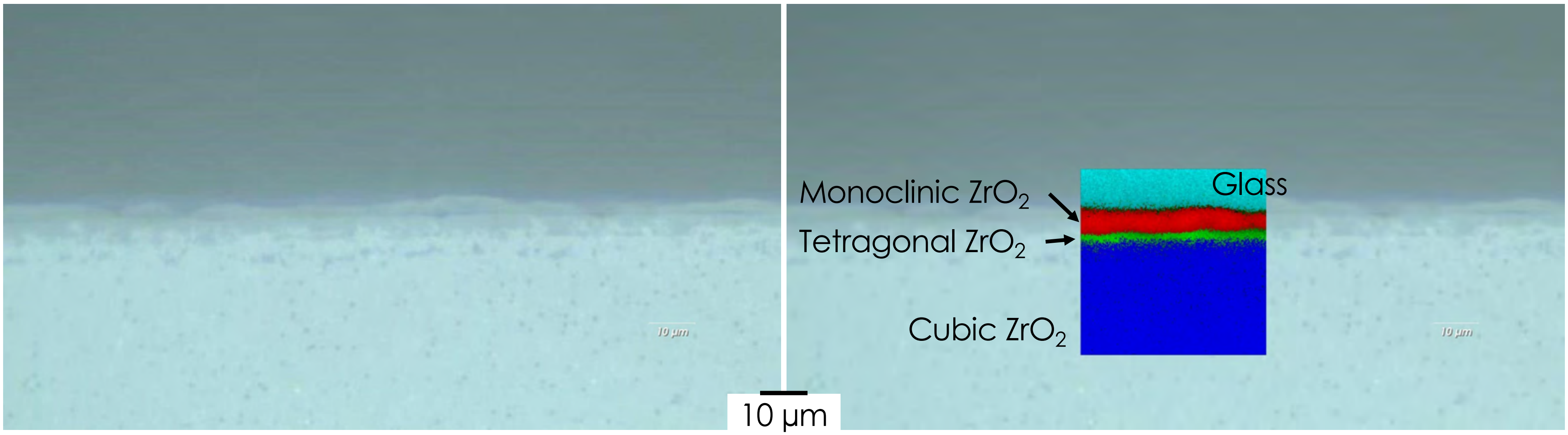

The diffusion of yttria into the glass, results in a transformation of the substrate from cubic to tetragonal to monoclinic ZrO_2.

Lara-Curzio et al. (2020)

Additional information about the characterization of these two multi-component silicate glasses can be obtained by contacting:

Edgar Lara-Curzio
laracurzioe@ornl.gov

Lara-Curzio et al. (2020)

Microstructural characterization of multi-component silicate glasses

- ORNL is compiling the results of this extensive study into a report and journal publications.
- Analysis of the results will provide information on the kinetics of crystallization of G6 and SCN glasses as a function of substrate (YSZ or Al_3O_3) and environment (air or H_2+H_2O+N_2)

Lara-Curzio et al. (2020)

• Additive manufacturing of SOFC materials and structures

- ORNL is developing slurries for the deposition of NiO-YSZ, YSZ and cathode materials.
- The focus has been on high-solid contents
- Rheology of slurries

Lara-Curzio et al. (2020)

Alternative Geometries

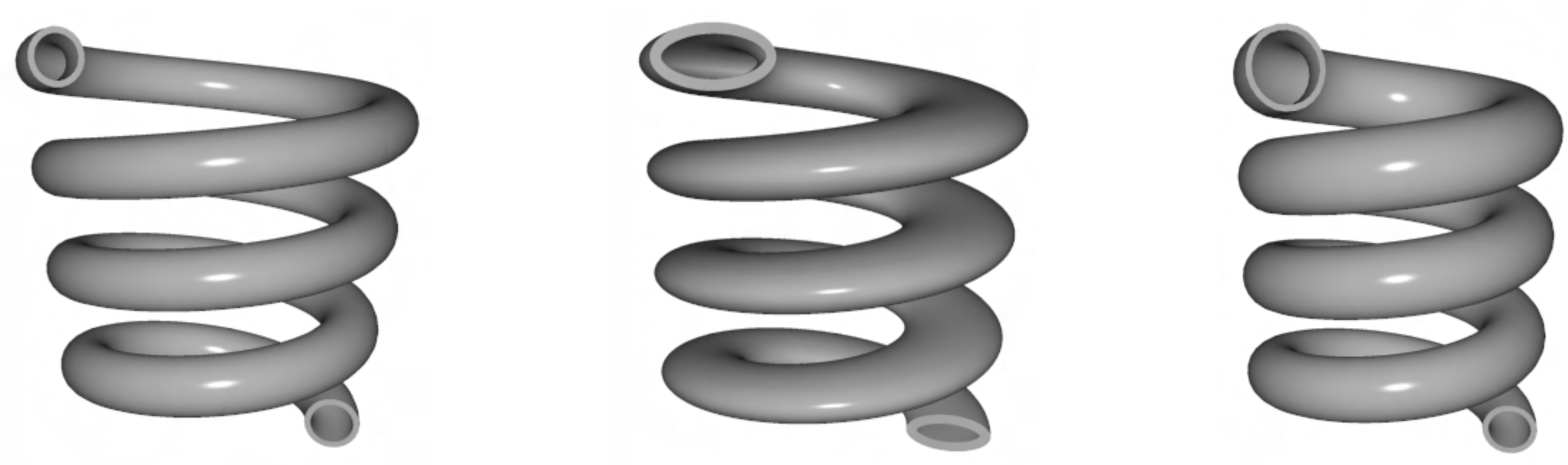

SOFCs don't have to be planar or straight tubes

Lara-Curzio et al. (2020)

Rheology of 8YZ/NiO/Pore Former Showed Complex Flow Behavior – more refinement required

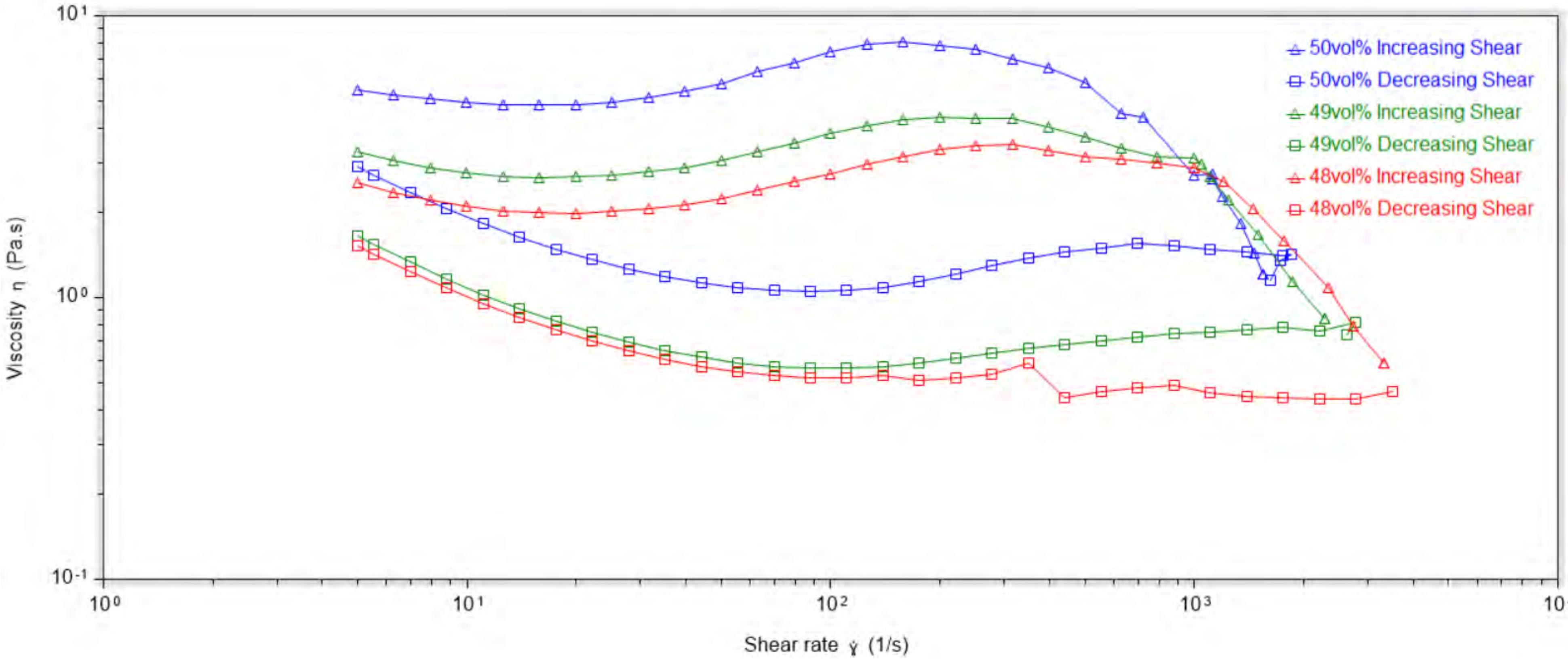

Lara-Curzio et al. (2020)

Zeta Potential

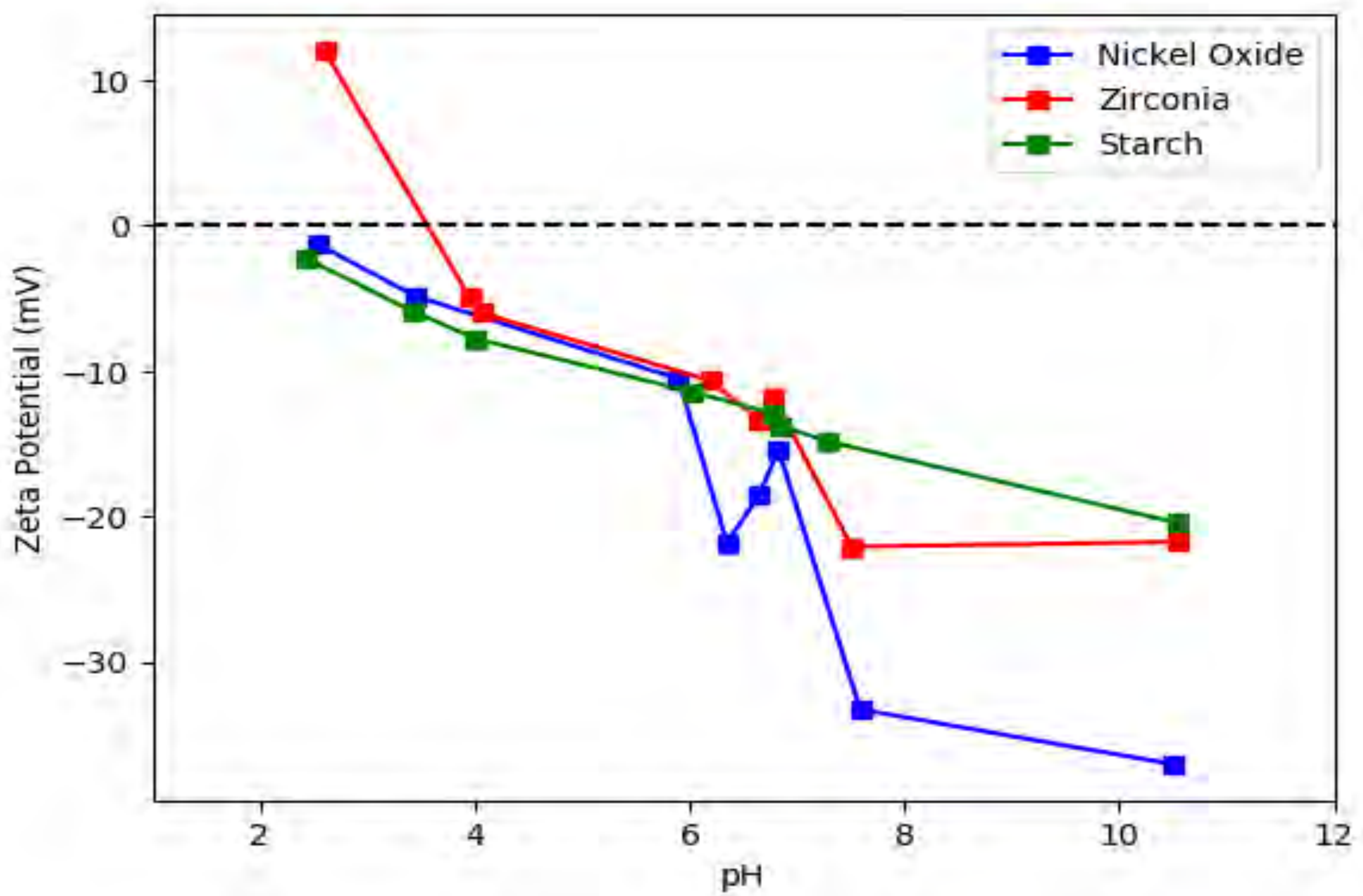

Materials' surface charges are compatible over a wide pH range if aqueous solution chemistries are utilized

Lara-Curzio et al. (2020)

Particle Size Distribution

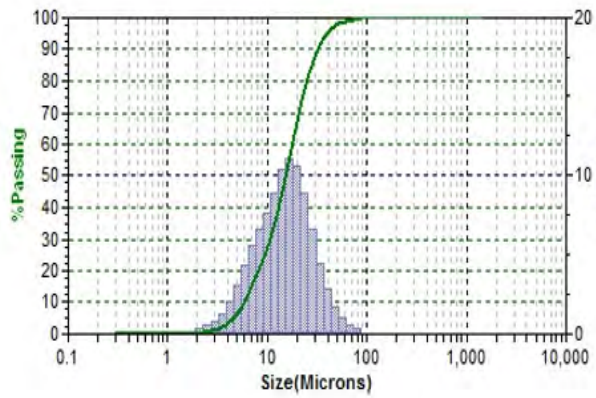

Nickel (II) Oxide
15.16 microns

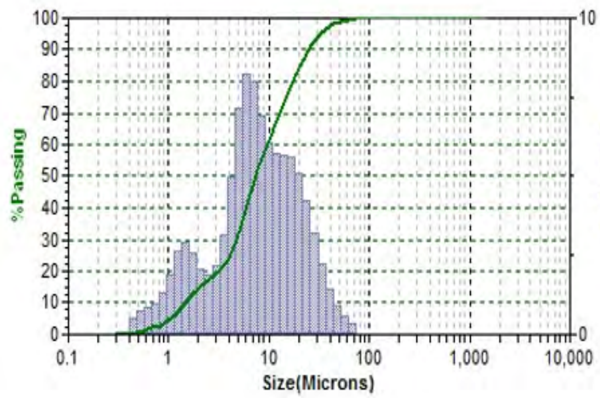

Rice Starch
1.234 microns
8.83 microns

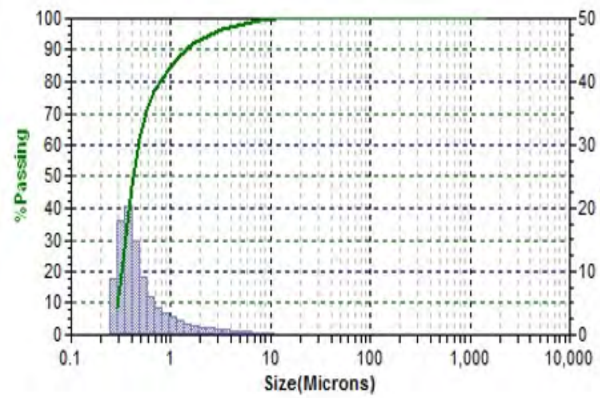

8YZ
422 nm

Lara-Curzio et al. (2020)

- **Additive manufacturing of SOFC materials and structures**

  - Activities are on hold because of COVID-19

Lara-Curzio et al. (2020)

• Summary and Future Activities

- A detailed analysis of the anomalous temperature-dependence of residual stresses in NiO-YSZ/YSZ bilayers has been completed. The analysis provides an explanation for the anomalous behavior based on transformations experienced by both NiO and YSZ as a function of temperature.
- A report documenting detailed characterization of multi-component silicate glasses as a function of time of exposure in SOFC-relevant environments is being completed
- Work on the development of new design methodologies and fabrication techniques for SOFCs continues.

Lara-Curzio et al. (2020)